PNAS
www.pnas.org

Supplementary Information for

The circadian clock of CD8 T cells modulates their early response to vaccination and the rhythmicity of related signaling pathways

Chloé C. Nobis, Geneviève Dubeau Laramée, Laura Kervezee, Dave Maurice De Sousa, Nathalie Labrecque and Nicolas Cermakian

Corresponding authors:
Nathalie Labrecque, Email: nathalie.labrecque@umontreal.ca
Nicolas Cermakian, Email: nicolas.cermakian@mcgill.ca

This PDF file includes:

Supplementary Materials and Methods
Captions for Datasets S1 to S3
Table S1
Figs. S1 to S10
References for SI reference citations
Statistical Details

Other supplementary materials for this manuscript include the following:

Datasets S1 to S3

Supplementary Materials and Methods

Mice. C57BL/6J mice (catalog number 000664), *Bmal1*$^{f/f}$ mice on C57BL/6J background (catalog number 007668), B6.SJL mice (B6.SJL-*Ptprc*^{a} *Pepc*^{b}/BoyJ, catalog number 002014) and PER2::LUC mice (catalog number 006852) were purchased from The Jackson Laboratory. OT-I *Rag2*$^{-/-}$ mice were purchased from Taconic (catalog numbers 2334-F, 2334-M). The latter 3 strains were then maintained as a breeding colony at the Douglas Institute animal facility. *E8I*-Cre$^{+/-}$ mice (C57BL/6-Tg(Cd8a-cre)1Itan/J (1) were obtained from Dr. Michel Tremblay (McGill University). *Bmal1*$^{+/-}$ mice (C57BL/6 background) were obtained from Dr. Florian Storch (McGill University) and bred to obtain *Bmal1*$^{+/+}$ and *Bmal1*$^{-/-}$ mice. (C57BL/6 X B6.SJL)F_1 mice (CD45.1/CD45.2) were obtained from Dr. Simona Stäger (INRS-Institut Armand-Frappier). *Bmal1*$^{f/f}$ and *E8I*-Cre$^{+/-}$ mice were bred to obtain *E8I*-Cre$^{+/-}$ *Bmal1*$^{f/f}$ (mice deficient for *Bmal1* in mature CD8 T cells, Δ/Δ) and their littermates *E8I*-Cre$^{-/-}$ *Bmal1*$^{f/f}$ (mice with *Bmal1* in all tissues, f/f). Genotyping of mice was as described: *Bmal1* KO (2), *Bmal1*$^{f/f}$ (3), *E8I*-Cre (1); in the case of *E8I*-Cre, in some cases, we genotyped the mice by flow cytometry, since *E8I*-Cre^{+} mice express GFP. All mice were housed at the animal facility of the Douglas Mental Health University Institute, in a pathogen-free environment. Animal use was in accordance with the guidelines of the Canadian Council of Animal Care and was approved by the Douglas Institute Facility Animal Care Committee.

Flow cytometry. Details of the antibodies and other reagents used for flow cytometry can be found in **Table S1**. Flow cytometry was performed on either a FACSCalibur or LSRFortessa (BD Biosciences), and analyzed using FlowJo software (FlowJo, LLC).

Bioluminescence recordings. BMDCs were prepared from bone marrow of PER2::Luciferase mice (4). CD8 T cells were isolated from spleens of PER2::Luciferase mice using EasySep™ mouse CD8a positive selection kit (Stemcell technologies, catalogue #18953), and purity of cells was confirmed to be above 95%. Two million BMDCs or 8 million CD8 T cells were seeded in 35 mm petri dishes, and their clocks synchronized by treatment with a medium composed of 50% RPMI and 50% of horse serum for 1 h at 37°C (5), which was then replaced with RPMI containing 0.1 mM luciferin but devoid of red phenol (also including 10% FBS and 1 ng/mL IL-7 for the CD8 T cells). Bioluminescence was recorded in a Lumicycle 32 equipment (Actimetrics).

BMDC migration assay. Ten million BMDCs generated from either *Bmal1*$^{+/+}$ or *Bmal1*$^{-/-}$ (full body KO) mice were stained with 5 μM of CFSE for 10 min, and injected i.v. in congenic B6.SJL mice at CT6. Four hours post injection, spleens were harvested to analyze the amount of dendritic cells that migrated in the tissue. Spleens were digested with 400 U/mL collagenase D for 30 min, then splenocytes were washed with RPMI 10% FBS and stained with anti-CD11c and anti-CD45.2 antibodies prior to flow cytometry. In other experiments, the same protocol was used but with B6.SJL BMDCs injected into *E8I*-Cre$^{+/-}$ *Bmal1*$^{f/f}$ or their Cre-less littermates.

Locomotor activity analysis. Mice were housed individually in cages equipped with running wheels, with ad libitum food and water. Cages and bedding were changed every other week at Zeitgeber time 13 (i.e. 1 h after lights off). ClockLab software (Actimetrics) was used for wheel-running data collection and analyses. Data were recorded for at least 15 days under a 12-h light: 12-h dark (LD) cycle followed by at least 15 days under constant darkness (DD). We used the data of the last 10 days in DD to determine the free-running period using chi-square periodogram.

Bone marrow transplantation. Naive mice have a low number of CD8 T cells that are specific for a particular antigen (only 50-200). Although these cells will massively expand following antigenic recognition, their detection is very difficult at early time points such as day 3 as they will only have started to expand and as such, they will be difficult to detect with tetramer staining at this early stage of the response. The only way to detect CD8 T cell response at this early stage requires to increase the frequency of antigen-specific T cells. Therefore, to assess the early CD8 T cell response, we aimed to use a mouse model where K^{b}-OVA-specific T cells would be enriched. The OT-I *Rag2*$^{-/-}$ mice have only one type of T cell receptor, with high affinity to K^{b}-OVA. Transplanting mixed bone marrow cells where OT-I cells represent 1% (as opposed to about 0.001% of OVA-specific cells in a normal C57BL/6 mouse) creates chimera mice which such an enriched T cell population. B6.SJL host mice (CD45.1) received 900 rad whole-body X-ray irradiation (RAD SOURCE Technologies RS2000) to achieve ablation of host hematopoietic cells. They were treated with antibiotics (Baytril, Bayer Healthcare) 3 days prior and for 3 weeks after irradiation. Immediately after irradiation the mice received 5x10^{6} bone marrow cells (1% from OT-I *Rag2*$^{-/-}$ mice [CD45.2], 99% from (C57BL/6 X B6.JSL)F$_{1}$ mice [CD45.1/CD45.2]). Six weeks later, bone marrow reconstitution was assessed in PBMCs purified from whole blood by Ficoll gradient purification, stained for CD45.1, CD45.2, CD8 and CD44. DC-OVA or DC-LPS vaccination was done at either CT6 or CT18 (as described above), in two separate experiments, 15 and 16 weeks after reconstitution. Three days post vaccination at the same time points as vaccination, mice were sacrificed,

spleen harvested, splenocytes stained for different markers in several panels, and analyzed by flow cytometry. The OVA-specific CD8 T cells were identified as CD45.1$^-$ CD45.2$^+$, and the non OVA-specific CD8 cells as CD45.1$^+$ CD45.2$^+$ (host cells were CD45.1$^+$ CD45.2$^-$). To assess phosphorylated S6 and AKT, splenocytes were rested in RPMI 1640 1% FBS for 30 min at 37°C followed by restimulation with 2 µg/mL $OVA_{257-264}$ for 30 min at 37°C. Surface staining CD8, CD45.1 and CD45.2 was followed by cell fixation using Fixation/Permeabilization Solution Kit (BD Bioscience #554714) prior to intracellular staining with anti-pS6 and anti-pAKT antibodies.

Ex vivo stimulation of OT-I/SJL splenocytes. OT-I *Rag2*$^{-/-}$ and B6.SJL mice were sacrificed at either CT6 or CT18 and the spleens were harvested. Splenocytes were mixed to a 1:1 ratio, rested in RPMI 1640 1% FBS for 30 min at 37°C followed by stimulation with 2 µg/mL $OVA_{257-264}$ for 30 min at 37°C for pS6 analysis and 60 minutes for pAKT analysis. Surface staining for CD8, CD45.1 and CD45.2 was followed by cell fixation using the BD Bioscience fixation/permeabilization kit prior to intracellular staining with anti-pS6 and anti-pAKT antibodies. The OVA-specific CD8 T cells (from OT-I) were determined as CD45.1$^-$ CD45.2$^+$, and the non OVA-specific CD8 T cells (from B6.SJL) as CD45.1$^+$ CD45.2$^-$.

Reverse transcription quantitative PCR and immunoblotting. The spleen, liver and thymus from *E8I*-Cre$^{+/-}$ *Bmal1*$^{f/f}$ or their Cre-less littermates were harvested. CD8$^+$ T cells and then CD4$^+$ T cells were successively isolated using EasySep™ mouse CD8a and CD4 positive selection kits (STEMCELL technologies, catalog #18953 and 18952). The remaining splenocytes were considered as CD4$^-$ CD8$^-$ cells. Total RNA was extracted from CD8 and CD4 T cells using TRIzol reagent (Invitrogen) and cleaned using RNeasy MinElute Cleanup Kit (Qiagen). The RNA was reversed transcribed using High Capacity cDNA Reverse Transcription Kit (Applied Biosystems), followed by quantitative PCR on a QuantStudio 6 PCR System (Applied Biosystems) using GoTaq qPCR Mastermix (Promega) with the following primers: *Bmal1* forward CCTAATTCTCAGGGCAGCAGAT, reverse TCCAGTCTTGGCATCAATGAGT, *Ef1α* (control gene) forward TGCCCCAGGACACAGAGACTTCA, reverse AATTCACCAACACCAGCAGCAA.
Proteins were extracted from CD8$^+$ and CD4$^+$ T cells, CD4$^-$ CD8$^-$ splenocytes, liver and thymus using RIPA lysis buffer. Immunoblotting was done using the following antibodies: anti-BMAL1 (Novus Biologicals, NB100-2288), HRP anti-rabbit IgG (secondary for BMAL1; Millipore Sigma, A9044), anti-Actin (Millipore Sigma, A5441), HRP anti-mouse IgG (secondary for Actin; Cedarlane, 111-035-144).

Captions for Datasets

Dataset S1. List of genes and RAIN analysis. The full list of genes is provided, along with the results of the RAIN analysis, including the p-value, FDR and rhythm parameters. FDR < 0.1 was considered statistically significant; at this cut off, all uncorrected p-values were below 0.006. See file Dataset_S1.csv.

Dataset S2. Cosinor analysis of rhythmic transcripts in CD8 T cells. Cosinor analysis was performed for the 786 genes found as rhythmic in the RAIN analysis. The phase according to the cosine fit as well as the phase bin are provided for each transcript. See file Dataset_S2.csv.

Dataset S3. Results of the GenExplain analysis. The lists of upstream master regulators, downstream effectors and transcription factors with enriched binding elements are provided for the groups of rhythmic genes peaking at each of the different time points (time bins from cosinor analysis). See file Dataset_S3.csv.

Table S1. Antibodies and other reagents for flow cytometry

Product	Clone	Fluorophore	Supplier	Experiments
CD8a	5.3-6.7	PeCy7	Biolegend	chimeras and ex vivo stimulations
CD8a	5.3-6.7	PerCP	Biolegend	all except chimeras/ex vivo
CD44	IM7	APC	Biolegend	all except chimeras/ex vivo
CD44	IM7	APC Fire	Biolegend	chimeras and ex vivo stimulations
CD44	IM7	FITC	Biolegend	all except chimeras/ex vivo
IFNγ	XMG1.2	FITC	Biolegend	IFNγ stains
IFNγ	XMG1.2	APC	Biolegend	IFNγ stains
Vβ5.1/5.2	MR9-4	FITC	Biolegend	Vβ stains
CD45.1	A20	BV421	Biolegend	chimeras and ex vivo stimulations
CD45.1	A20	FITC	Biolegend	chimeras
CD45.2	104	PE	Biolegend	chimeras and DC migration
CD45.2	104	AF700	Biolegend	chimeras
CD62L	MIL-14	BV421	Biolegend	chimeras
IRF4		PE	Biolegend	chimeras
CD69	H1.2F3	APC	Biolegend	chimeras
CD5	53-7.3	PerCP	Biolegend	chimeras
CD98	RL388	AF647	Biolegend	chimeras
CD71	RI7217	BV421	Biolegend	chimeras
I-A^b	AF6-120.1	FITC	Biolegend	I-A^b stains
CD86	GL-1	PE	Biolegend	CD86 stains
CD11c	N418	APC	Biolegend	CD11c stains
K^b	AF6-88.5	Biotin	Biolegend	K^b stains

Streptavidin		PerCP	Biolegend	K^b stains
K^b-OVA	25-D1.16		in-house	K^b-OVA stains
IgG-I	RMG1-1	PE	Biolegend	2^{ary} for K^b-OVA stains
Annexin V		FITC	Biolegend	apoptosis stains
7-AAD			Biolegend	apoptosis stains
pS6 (Ser235/236)	cupk43k	PE	eBioscience	chimeras and ex vivo stimulations
pAKT (Ser473)	SDRNR	APC	eBioscience	chimeras and ex vivo stimulations
TetOVA		PE	in-house	TetOVA stains
CFSE			Biolegend	DC migration

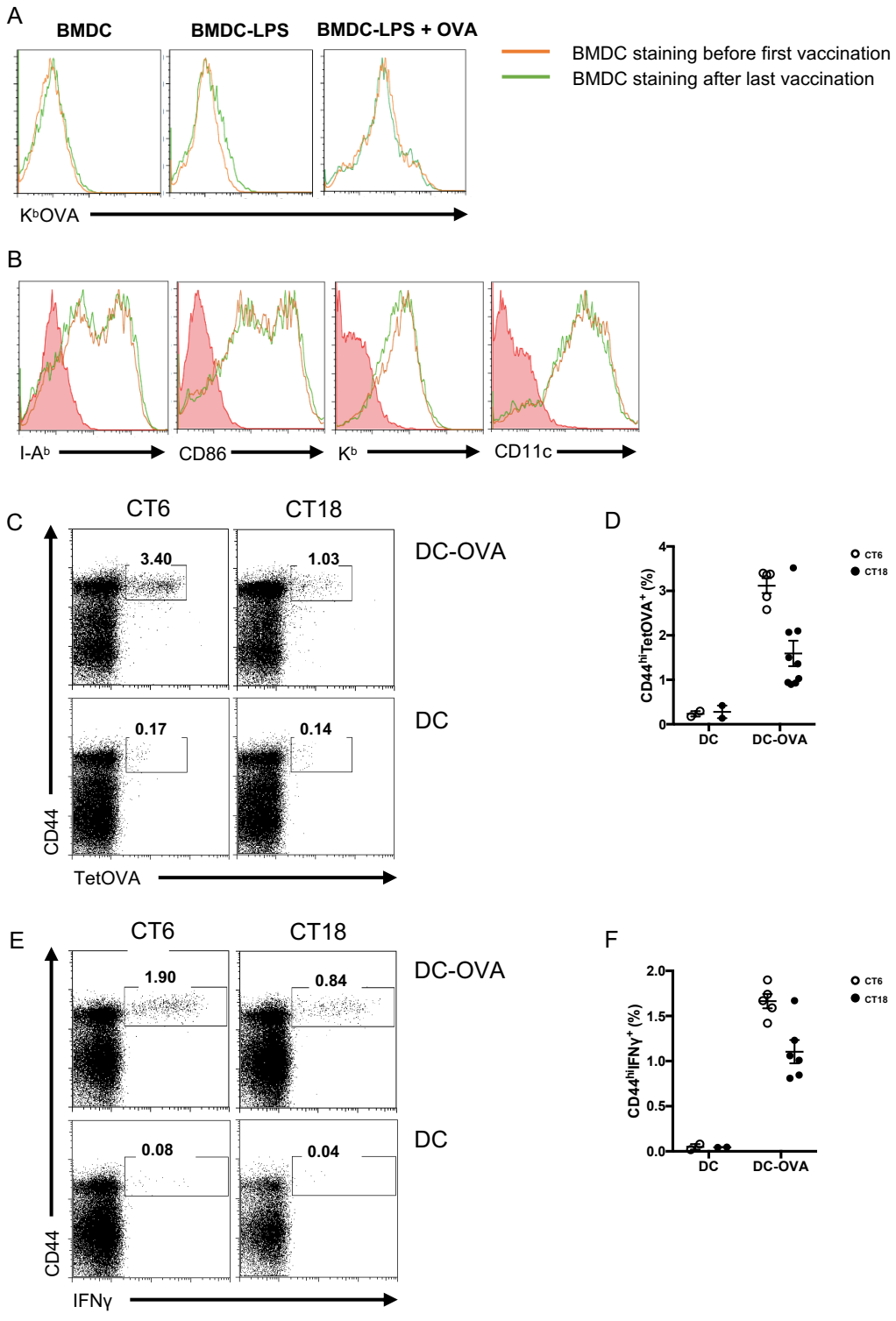

(See legend of Fig. S1, next page)

Fig. S1. Bone marrow-derived dendritic cell (BMDC) phenotyping and analysis of OVA-responsive CD8 T cells. *(A, B)* Representative histograms of *(A)* the BMDC loading with OVA, using anti-K^b-OVA staining and *(B)* the BMDC activation using anti-I-A^b, anti-CD86, anti-K^b and anti-CD11c antibodies. The FACS plots depict a comparison of the BMDCs either prior to the first vaccination (orange line) or after the last vaccination (green line). *(C-F)* Analysis of the CD8 T cell response to DC-OVA. Representative dot plots *(C)* and quantification *(D)* of the expansion of OVA-responsive CD8 T cells using tetramer OVA (TetOVA) staining. Representative dot plots *(E)* and quantification *(F)* of the OVA-specific CD8 T cells that express IFNγ after *ex vivo* restimulation with OVA peptide. Data for DC-OVA (in *D* and *F*) are the same as in Fig. 1.

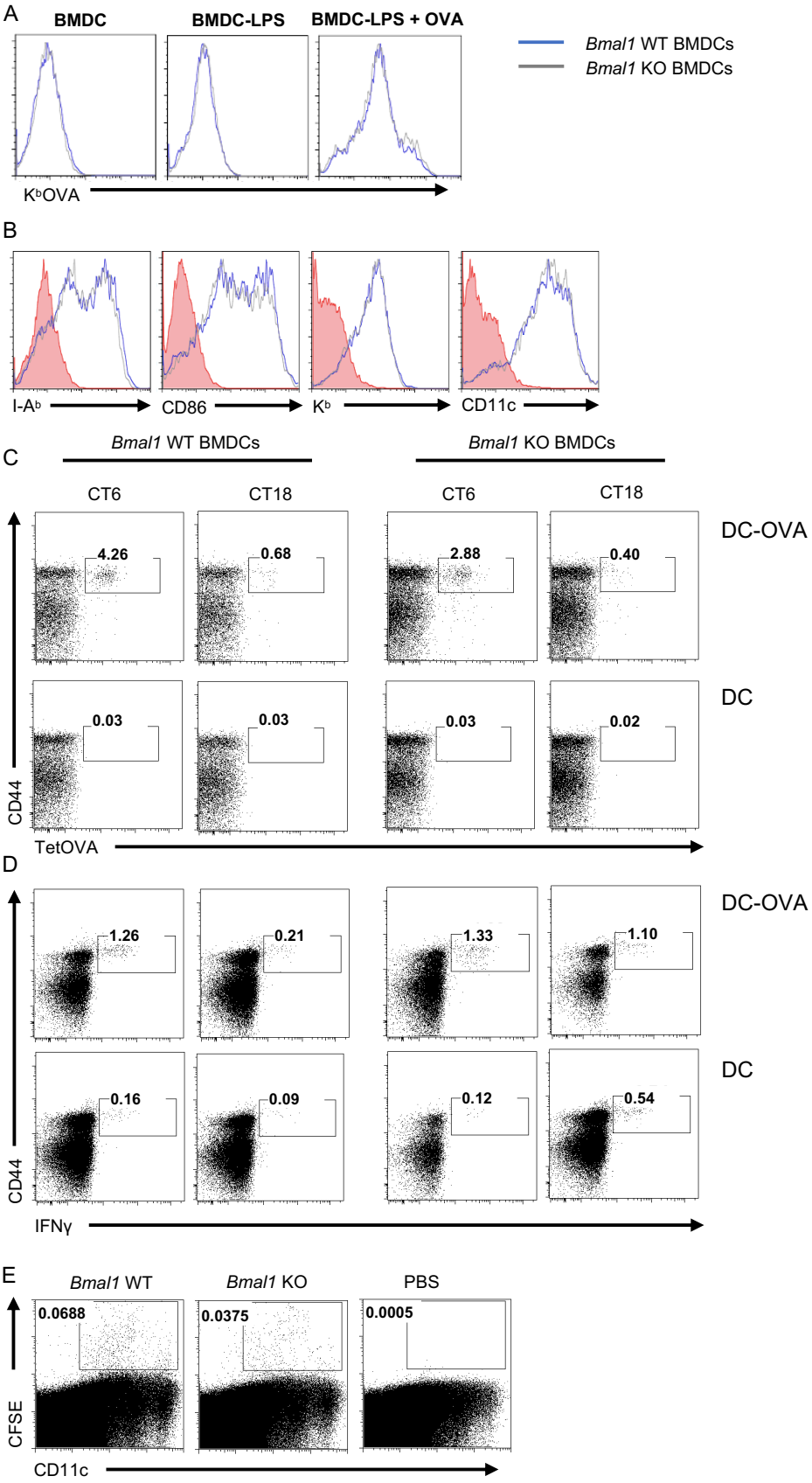

(See legend of Fig. S2, next page)

Fig. S2. *Bmal1* KO bone marrow-derived dendritic cell (BMDC) phenotyping and analysis of OVA-responsive CD8 T cells and DC migration. *(A, B)* Representative histograms of *(A)* the BMDC loading with OVA, using anti-K^b-OVA staining and *(B)* the BMDC activation using anti-I-A^b, anti-CD86, anti-K^b and anti-CD11c antibodies. The FACS plots depict a comparison of either WT (blue line) or *Bmal1* KO (grey line) BMDCs. *(C, D)* Gating strategy for the analysis of the CD8 T cell response to WT or *Bmal1* KO DC-OVA in WT mice. Representative dot plots of *(C)* CD8 T cell expansion using tetramer OVA staining (TetOVA) and of *(D)* the OVA-specific CD8 T cells that express IFNγ after *ex vivo* restimulation with OVA peptide. *(E)* Representative dot plots for the analysis of DC migration to the spleen, by measurement of $CFSE^+CD11c^+$ splenocytes in B6.SJL mice injected with WT or *Bmal1* KO DC-OVA.

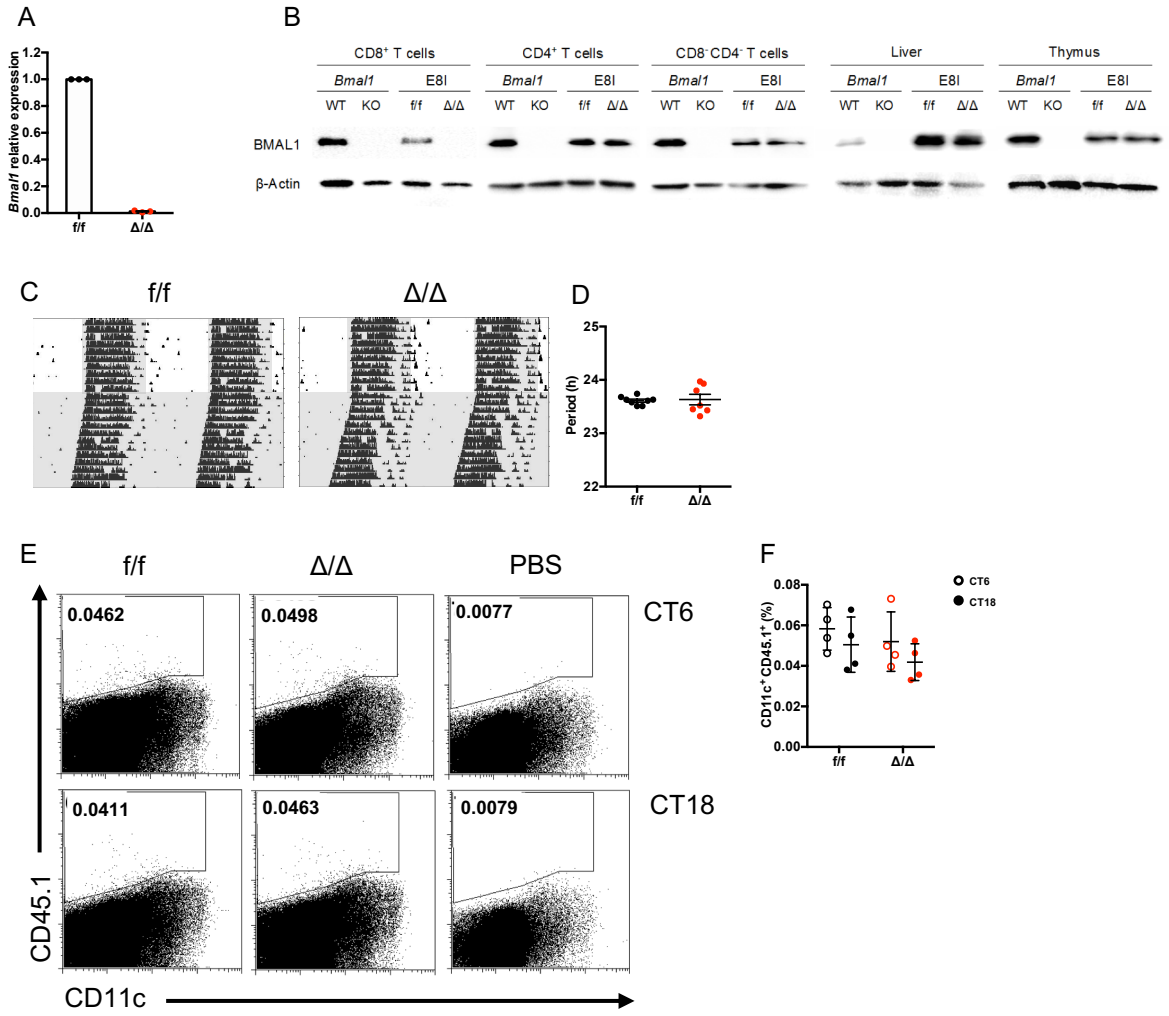

Fig. S3. Characterization of the CD8 T cell-specific *Bmal1* KO (*E8I*-Cre *Bmal1*$^{f/f}$) mice. *(A) Bmal1* gene expression in mature CD8 T cells isolated from spleens of *E8I*-Cre *Bmal1*$^{f/f}$ mice (CD8 T cell-specific *Bmal1* KO mice, Δ/Δ) and controls without *E8I*-Cre (f/f) by quantitative PCR. *(B)* BMAL1 protein expression levels (and β-Actin as control) analyzed by immunoblotting on CD8$^+$, CD4$^+$ and CD8$^-$CD4$^-$ T cells isolated from spleens, and liver and thymus, from full body *Bmal1* KO mice and WT controls (left 2 lanes for each cell type/tissue) and from *E8I*-Cre *Bmal1*$^{f/f}$ mice (Δ/Δ) and controls (f/f) (right 2 lanes for each cell type/tissue). *(C, D)* Analysis of the wheel-running behavior of *E8I-Cre Bmal1*$^{f/f}$ (Δ/Δ) and controls (f/f) for 10 days in LD followed by 13 days in DD. Actograms in *(C)* are double-plotted. *(D)* shows the free-running period of the mice (n = 7-8/group, t test n.s.). *(E, F)* DC migration to the spleen, by measurement of CD45.1$^+$ splenocytes (BMDCs from B6.SJL mice) in *E8I*-Cre *Bmal1*$^{f/f}$ mice (Δ/Δ) and controls (f/f). *(E)* Representative dot plots, *(F)* Quantification in 4 mice per genotype and CT (Two-way ANOVA, n.s.). See SI Appendix, Statistical Details for more information on statistics.

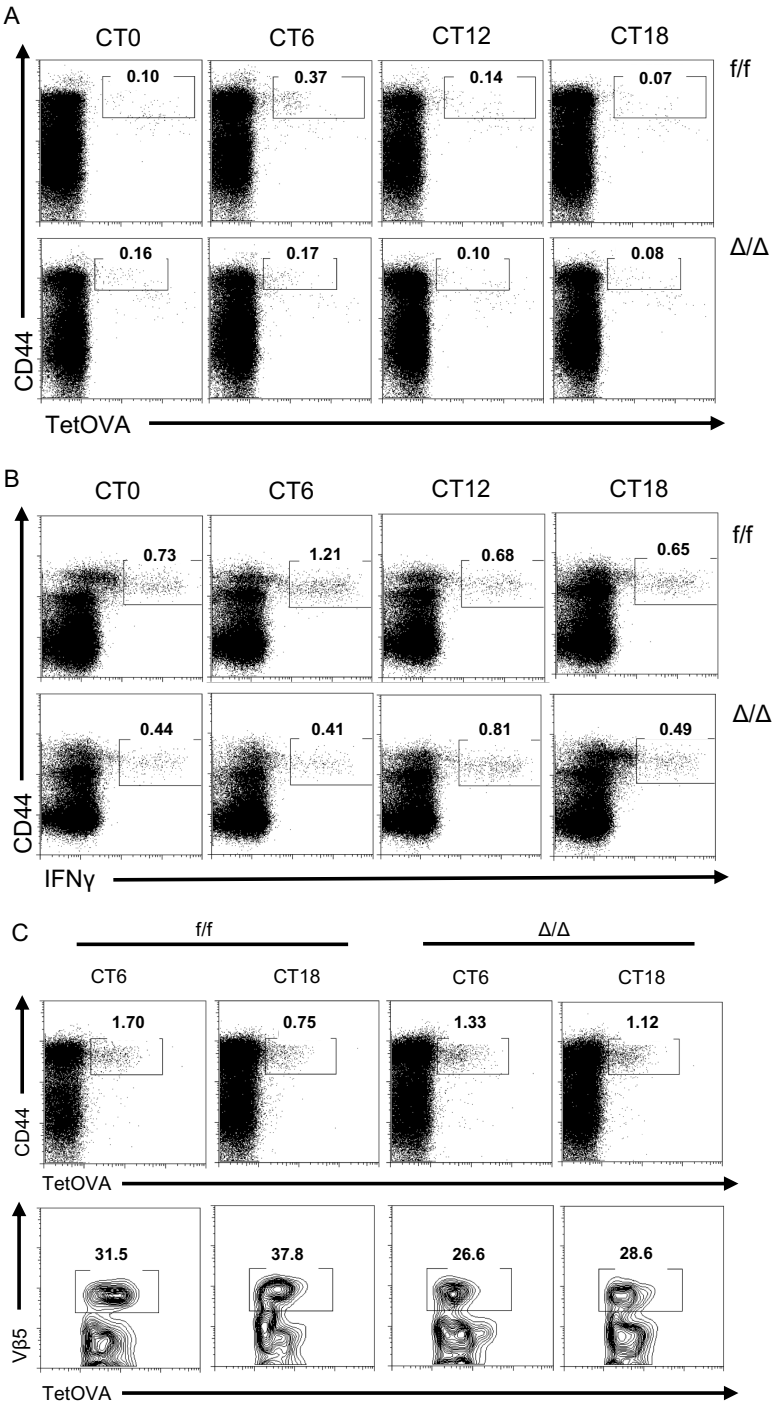

Fig. S4. Analysis of the CD8 T cell response to DC-OVA in CD8 T cell-specific *Bmal1* KO (*E8I*-Cre *Bmal1*$^{f/f}$) mice. *(A, B)* Gating strategy for the analysis of the CD8 T cell response to DC-OVA in *E8I*-Cre *Bmal1*$^{f/f}$ mice (CD8 T cell-specific *Bmal1* KO mice, Δ/Δ) and controls without *E8I*-Cre (f/f). Representative dot plots of *(A)* CD8 T cell expansion using tetramer OVA staining (TetOVA) and of *(B)* the OVA-specific CD8 T cells that express IFNγ after *ex vivo* restimulation with OVA peptide. *(C)* Gating strategy of the analysis of the expansion and the level of Vβ5$^+$ cells among the TetOVA$^+$ cells in Δ/Δ and f/f mice, 7 days after vaccination with DC-OVA at different CT6/18.

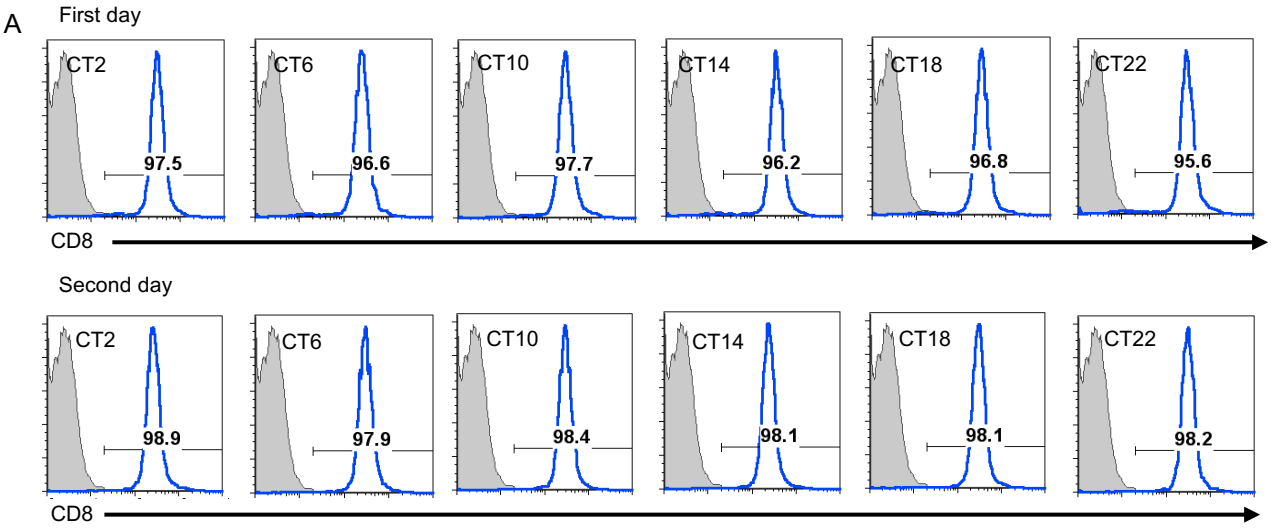

B

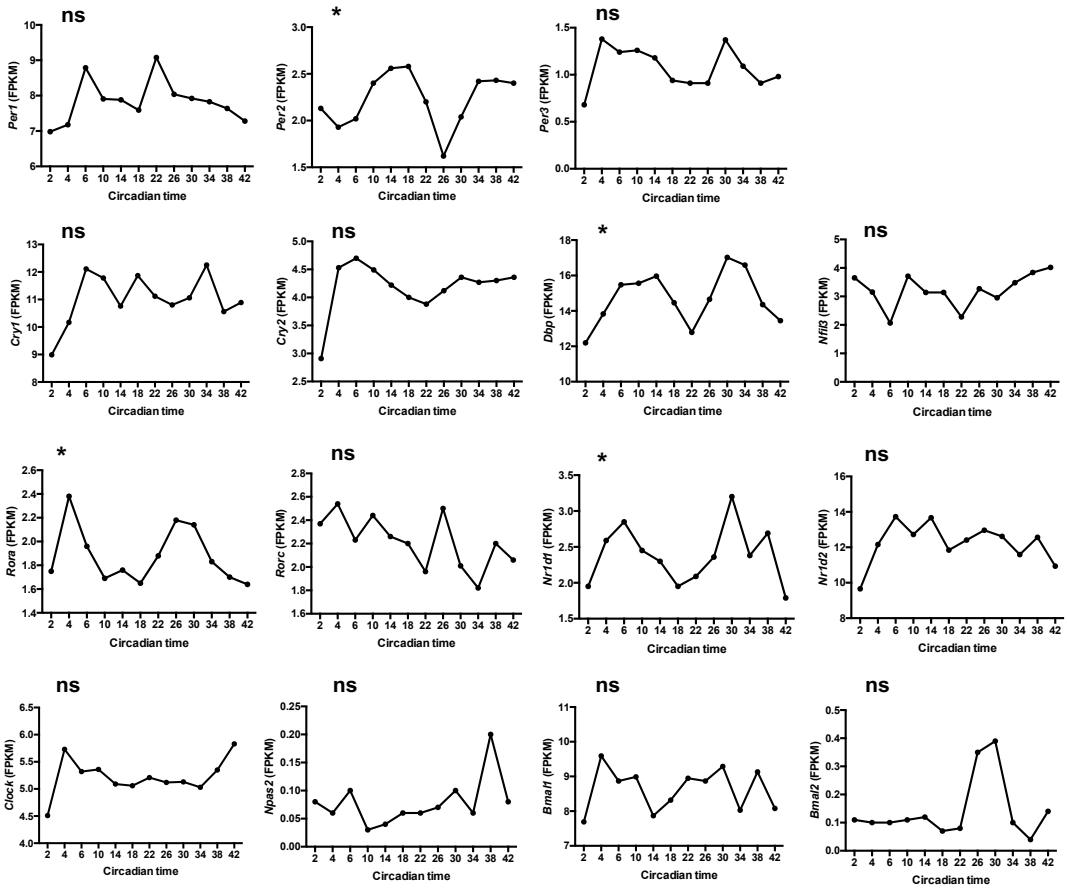

(See legend of Fig. S5, next page)

Fig. S5. Isolation of CD8 T cells for the transcriptomic experiment and clock gene expression. *(A)* Verification of the purity of the $CD8^+$ T cells (blue lines) isolated from lymph nodes harvested at 12 different circadian times over two days (unlabeled control in grey). *(B)* Expression profiles of 15 clock genes in CD8 T cells (from the RNA-seq data). *, significant rhythmicity as per criterion (FDR < 0.1); nr, non-significant rhythmicity.

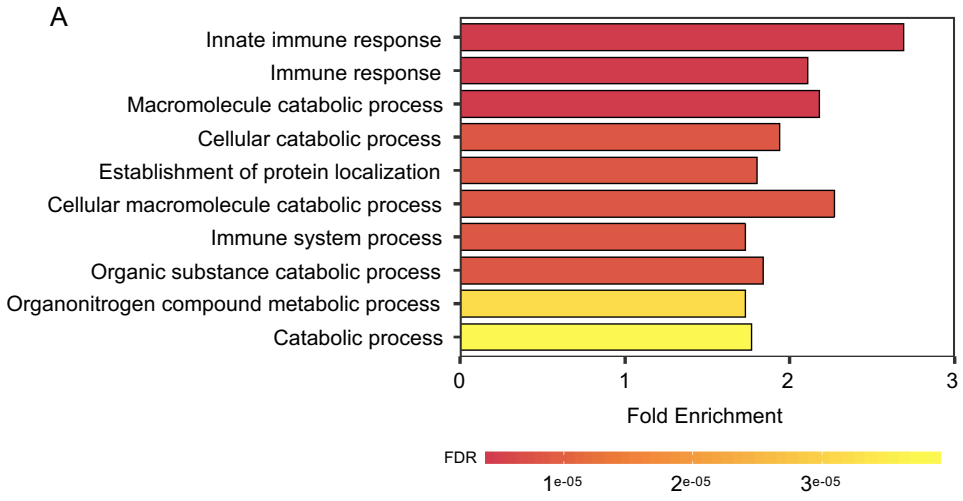

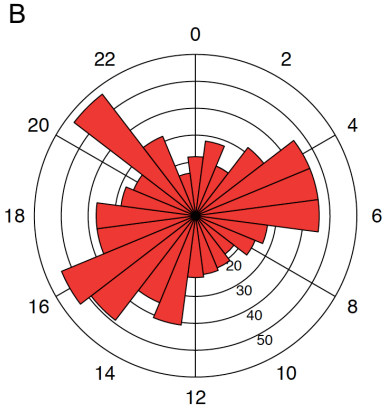

C

Phase	Transcription factor	P-value
CT2	**OCT**	**0.047**
CT6	**-**	
CT10	**IRF4** **BLIMP1**	**0.028** **0.030**
CT14	**-**	
CT18	**-**	
CT22	**-**	

Fig. S6. Circadian transcriptomic analysis of CD8 T cells. *(A)* Gene ontology analysis of rhythmic genes in CD8 T cells, using WEB-based GEne SeT AnaLysis Toolkit. *(B)* Phase distribution of the rhythmic genes, using phases determined by cosinor analysis. *(C)* Transcription factors whose elements are significantly enriched in the genomic region of the CD8 T cell rhythmic genes, determined using GenExplain platform.

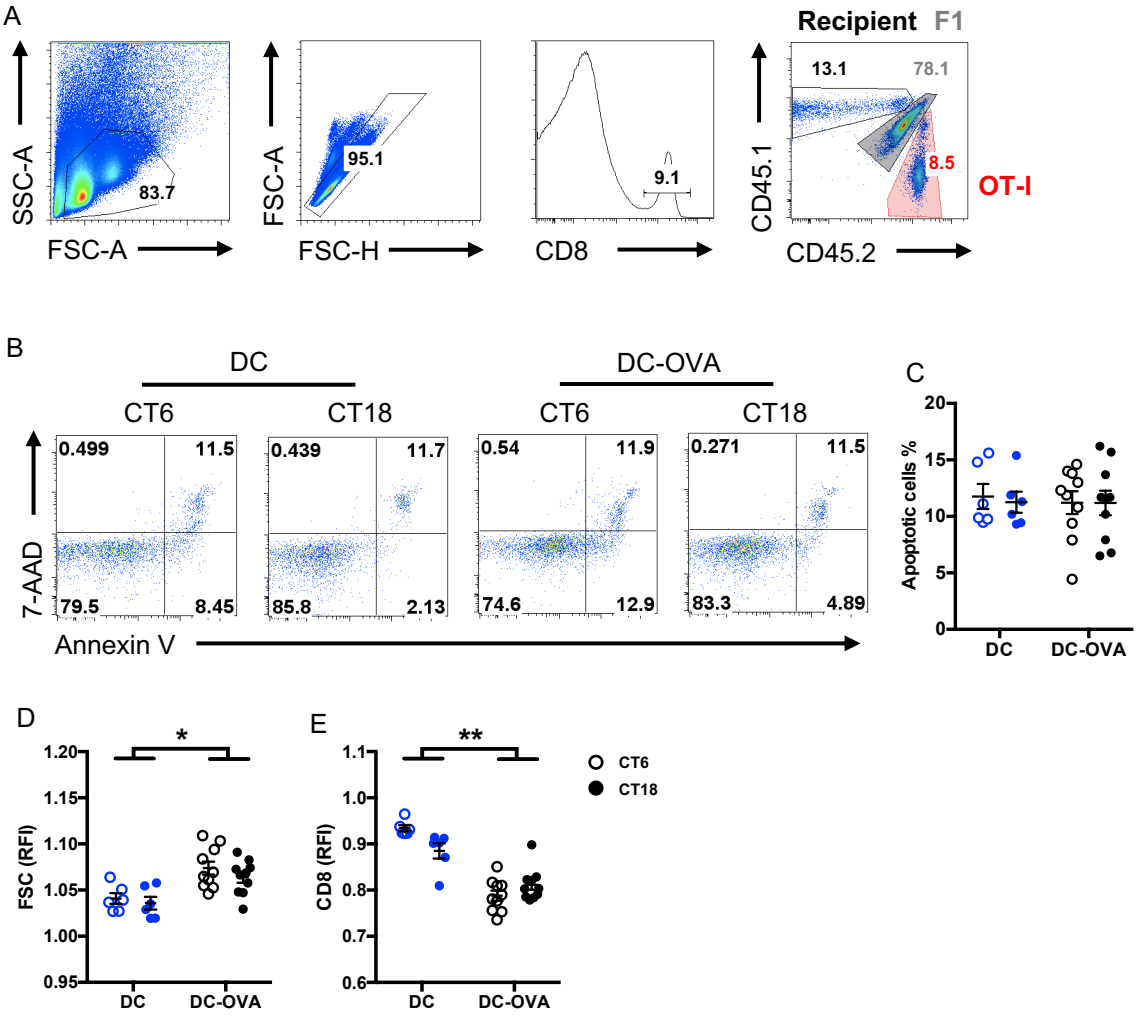

Fig. S7. Analysis of cell size, CD8 levels and apoptosis in bone marrow chimeric mice. Analysis of the same samples as in Fig. 5. *(A)* Gating strategy and representative dot plots or histograms for CD8+ T cell, and for OT-I cells (red-shaded gate) and non OVA-specific CD8 T cells (F1, grey-shaded gate). *(B, C)* Evaluation of apoptosis using Annexin V and 7-AAD staining. *(B)* Representative dotplots, *(C)* Quantification of apoptotic cells (Annexin V^+7-AAD^+) among OT-I cells. *(D, E)* Relative mean fluorescence intensity (ratio between OT-I [$CD8^+CD45.1^-CD45.2^+$] cells and non OVA-specific CD8 T cells [$CD8^+CD45.1^+CD45.2^+$] cells) for *(D)* cell size (FSC) and *(E)* CD8 levels. In *(C-E)*, data are pooled from 2 independent experiments with similar results, n = 6-10 mice/group. Data are shown for individual mice, as well as mean ± SEM. Two-way ANOVA with Bonferroni post hoc test where applicable. There was an interaction for FSC *(D)* but only an effect of treatment for CD8 *(E)*. For simplicity, only the post hoc for the effect of treatment are shown in the figure, * $p < 0.05$, ** $p < 0.01$. See SI Appendix, Statistical Details for more information on statistics.

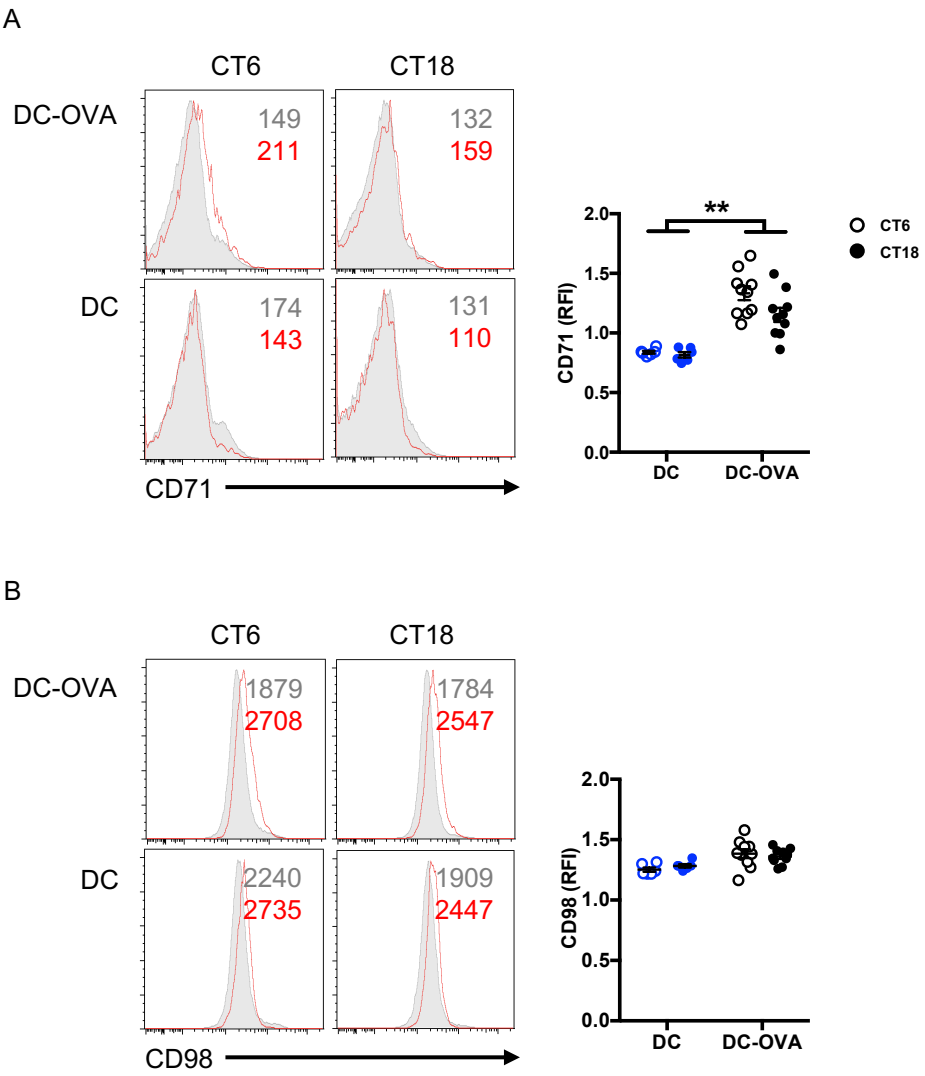

Fig. S8. Analysis of metabolic markers in bone marrow chimeric mice. Analysis of the same samples as in Fig. 5. *(A)* CD71, *(B)* CD98. In each panel, representative FACS histograms are shown on the left (OT-I cells in red, F1 cells in grey; see Fig. S6A for gating of these populations). The number represent the geometric mean fluorescence of the corresponding marker analyzed. On the right of each panel, the relative mean fluorescence intensity (ratio between OT-I [$CD8^+CD45.1^-CD45.2^+$] cells and non OVA-specific CD8 T cells [$CD8^+CD45.1^+CD45.2^+$] cells) is shown, for individual mice as well as mean ± SEM, with 6-10 mice per group. Two-way ANOVA with Bonferroni post hoc test where applicable; there was an effect of treatment in both cases, but post hocs were only significant for CD71, as illustrated in the figure, ** $p < 0.01$. See SI Appendix, Statistical Details for more information on statistics.

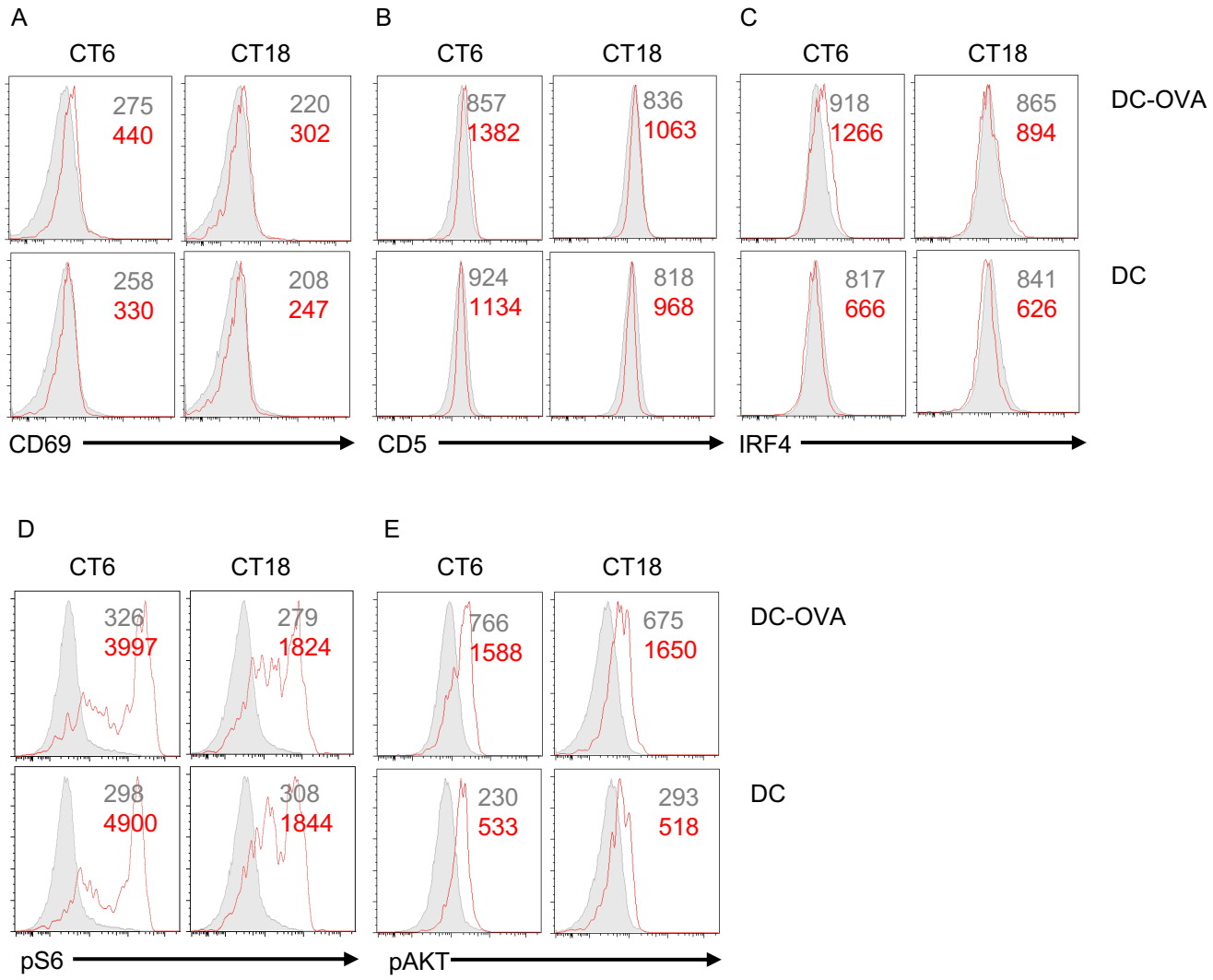

Fig. S9. Analysis of T cell activation markers in bone marrow chimeric mice. Analysis of the same samples as in Fig. 5. Representative FACS histograms are shown for activation markers: *(A)* CD69, *(B)* CD5 and *(C)* IRF4; and phospho-proteins: *(D)* pS6 and *(E)* pAKT). OT-I cells in red, F1 cells in grey; see Fig. S6A for gating of these populations. The number represent the geometric mean fluorescence of the corresponding marker analyzed. See Fig. 5B-F for the full data.

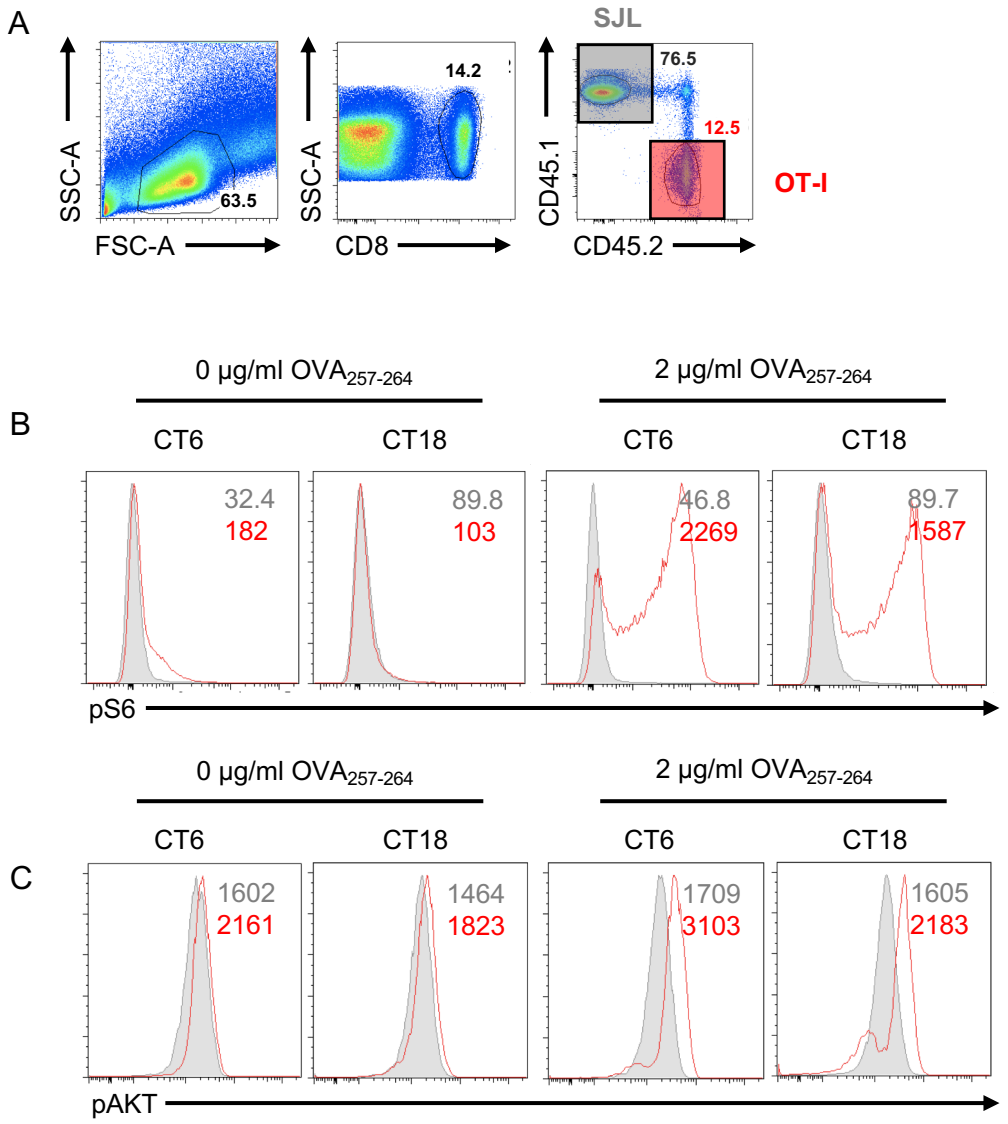

Fig. S10. Analysis of S6 and AKT phosphorylation *ex vivo*. OT-I (red-shaded gate) and non OVA-specific CD8 T splenocytes (SJL, grey-shaded gate) were cultured *ex vivo* and stimulated with OVA peptide, and analyzed for pS6 and pAKT. *(A)* Gating strategy for the different cell populations. *(B, C)* Representative histograms for pS6 *(B)* and pAKT *(C)* stainings. OT-I cells in red, SJL cells in grey. The number represent the geometric mean fluorescence of the corresponding marker analyzed. See Fig. 6 for the full data.

References for SI reference citations

1. Maekawa Y*, et al.* (2008) Notch2 integrates signaling by the transcription factors RBP-J and CREB1 to promote T cell cytotoxicity. *Nat Immunol* 9(10):1140-1147.
2. Bunger MK*, et al.* (2000) Mop3 is an essential component of the master circadian pacemaker in mammals. *Cell* 103(7):1009-1017.
3. Storch KF*, et al.* (2007) Intrinsic circadian clock of the mammalian retina: importance for retinal processing of visual information. *Cell* 130(4):730-741.
4. Yoo SH*, et al.* (2004) PERIOD2::LUCIFERASE real-time reporting of circadian dynamics reveals persistent circadian oscillations in mouse peripheral tissues. *Proc Natl Acad Sci U S A* 101(15):5339-5346.
5. Balsalobre A, Damiola F, & Schibler U (1998) A serum shock induces circadian gene expression in mammalian tissue culture cells. *Cell* 93(6):929-937.